A Nowcast/Forecast System for Coastal Ocean Circulation Using Simple Nudging Data Assimilation

JIA WANG

International Arctic Research Center–Frontier Research System for Global Change, University of Alaska Fairbanks, Fairbanks, Alaska

(Manuscript received 13 December 1999, in final form 6 October 2000)

ABSTRACT

This study describes the establishment of a Nowcast/Forecast System for Coastal Ocean Circulation (NFS-COC), which was run operationally on a daily basis to provide users ocean surface currents and sea levels that vary with synoptic winds, and seasonal and mesoscale variability intrinsic to the Florida Current. Based on the requirements of users, information about possible oil spills, trajectories, etc., is also provided by NFS-COC.

NFS-COC consists of two parts: a 3D ocean nowcast/forecast circulation model, Princeton Ocean Model (POM), and a 2D trajectory model. POM is automatically run to forecast ocean variables for up to 2 days under forcing of the Florida Current inflow/outflow and the predicted surface winds, which are automatically transferred (by ftp) from a file server at the National Meteorological Center (now known as the National Centers for Environmental Prediction). The winds from the mesoscale Eta Model are called Eta winds. Then the trajectory model is run to predict the path due to 1) the POM-predicted ocean surface currents, 2) wind drift due to the predicted Eta winds, and 3) turbulent dispersion based on a random flight (Markov process) model. The predicted surface trajectories can be used to estimate the physical transport of oil spills (and other drifting or floating objects) in the Straits of Florida and many other coastal seas. A simple data assimilation scheme (nudging to the volume transport) is designed into the NFS-COC, although some powerful data assimilation methods exist for assimilating other physical variables.

1. Introduction

For many scientific and practical purposes, a Nowcast/Forecast System for Coastal Ocean Circulation (NFS-COC) is essential to advance ocean science from the descriptive stage to a numerical prediction stage. In meteorology, numerical weather forecasts (Black 1994; Rogers et al. 1995) have been conducted operationally (and in the research model) for three decades now. In oceanography, numerical prediction has lagged behind due to the lack of process understanding, well-validated models, operational observational networks, data assimilation methods, and computational resources. The situation has now changed in all these regards, although observational networks are not yet fully adequate. However, their future development needs the impetus provided by a research system such as NFS-COC.

In conducting adaptive, process-oriented field experiments, it is important to have a good estimate of the regional circulation, which can be provided by a nowcast/forecast system. Similarly, in dealing with pollutants (e.g., oil spills), it is essential to have a good estimate of the transient circulation in order to predict likely spill trajectories due to advection and dispersion. A nowcast system consists, most fundamentally, of a circulation model, an observing system, and a data assimilation method.

The aim was to develop a coastal ocean nowcast/forecast system for the Straits of Florida with links to a regional mesoscale atmospheric model. Here the focus is placed on the ocean nowcast/forecast system with a simple data assimilation approach to the available observations. The Princeton Ocean Model (POM; Blumberg and Mellor 1987; Mellor 1996) was chosen because of its ability to deal with variable topography, density stratification, and thermohaline processes and its success in many other applications (Wang et al. 1994; Wang and Ikeda 1996; Wang and Mooers 1997; Mooers and Wang 1998; Wang et al. 1997). The most rudimentary data assimilation scheme, called ''nudging,'' will be used in this early stage. The approach includes continually operating a relatively coarse (but eddy resolving) grid nowcast system using operational (autonomous real-time) observations.

NFS-COC was designed for use in the Straits of Florida because the physics and observations of the Florida Current have been investigated to some extent. The circulation in the Straits of Florida is dominated by the Florida Current, which is largely in geostrophic balance,

Corresponding author address: Dr. Jia Wang, International Artic Research Center (IARC)–Frontier Research System for Global Change (FRSGC), University of Alaska, Fairbanks, P.O. Box 757335, Fairbanks, AK 99775-7335.
E-mail: jwang@iarc.uaf.edu

has an annual cycle of transport variation of ±3 Sv (Sv ≡ 10^6 m^3 s^{-1}) around a mean of 32 Sv, and meanders on the timescale of several days to a few weeks (Lee et al. 1985; Molinari et al. 1985; Schott et al. 1988; Johns and Schott 1987). It also sheds so-called spin-off eddies (Lee and Mayer 1977) and is associated with transient undercurrents (Duing and Johnson 1971) and countercurrents (Brooks and Niiler 1975; Lee et al. 1985; Leaman and Molinari 1987). It is influenced by local synoptic atmospheric forcing (Lee and Williams 1988) and tidal forcing (Mayer et al. 1984), and by variability in the Gulf of Mexico and to the east of the Bahamas. Occasionally, large mesoscale eddies enter the Straits of Florida from the Gulf of Mexico and continue to move downstream, decreasing in size due to shearing processes and effect of sloping topography (Wang and Ikeda 1997). Countercurrents, small mesoscale (spin-off) eddies, fronts, and onshore–offshore jets were detected by observations and numerical modeling (Wang and Mooers 1997).

NFS-COC is basically divided into two parts: the circulation model and the trajectory model. The circulation model uses (6-hourly) Eta winds (on a 80 km × 80 km grid), which are downloaded (by ftp) from the National Meteorological Center (now known as the National Centers for Environmental Prediction, NCEP) and interpolated onto the ocean model grid (Black 1994; Rogers et al. 1995). After the POM calculation, the surface currents (1-m depth) are extracted and served as the synoptic circulation pattern for the trajectory model. Then, trajectories are predicted for oil spills, fish eggs and larvae, etc.

Section 2 describes the two models, the ocean circulation model and the trajectory model, and the data assimilation scheme. Section 3 documents each element of the system, including C-shell script files, which automatically control NFS-COC. Section 4 displays and discusses some outputs and physical processes. Finally, progress is summarized and future work is outlined in section 5.

2. Description of the NFS-COC models

There are two models for the NFS-COC. POM first nowcasts and forecasts the ocean circulation pattern in the Straits of Florida (Wang and Mooers 1997). The surface trajectory model then predicts tracer paths under forcing of surface current, direct wind drift, and turbulent dispersion.

a. Ocean circulation model

The circulation model, POM, is a 3D, primitive equation model (Mellor 1996) in sigma (terrain following) coordinates. It has a free surface and uses a splitting technique for time integration of the barotropic (external) and baroclinic (internal) modes. The Coriolis parameter is held constant for the limited domain of the Straits of Florida. Only the density field is treated; that is, the temperature and salinity fields are not treated individually in this version.

Under the hydrostatic and Boussinesq approximations, the model is governed by the following equations (in Cartesian coordinates for simplicity):

$$\frac{\partial u}{\partial t} + L(u) - fv = -\frac{1}{\rho_o}\frac{\partial p}{\partial x} + \frac{\partial}{\partial z}\left(K_M\frac{\partial u}{\partial z}\right) + F_x, \quad (1)$$

$$\frac{\partial v}{\partial t} + L(v) + fu = -\frac{1}{\rho_o}\frac{\partial p}{\partial y} + \frac{\partial}{\partial z}\left(K_M\frac{\partial v}{\partial z}\right) + F_y, \quad (2)$$

$$\rho g = -\frac{\partial p}{\partial z}, \quad (3)$$

$$\frac{\partial u}{\partial x} + \frac{\partial v}{\partial y} + \frac{\partial w}{\partial z} = 0, \quad (4)$$

$$\frac{\partial \rho}{\partial t} + L(\rho) = \frac{\partial}{\partial z}\left(K_H\frac{\partial \rho}{\partial z}\right) + F_\rho, \quad (5)$$

where u, v, and w are the velocity components of the x (eastward positive), y (northward positive), and z (upward positive from the mean sea level) directions, respectively; ρ_o and ρ are the reference density and in situ density of water; g is the gravitational acceleration; p is the water pressure; and f is the Coriolis parameter. Here L is the nonlinear advection operator such that $L(\beta) = \partial(u\beta)/\partial x + \partial(v\beta)/\partial y + \partial(w\beta)/\partial z$; K_M is the vertical viscosity for mixing of turbulent momentum; F_x and F_y are the horizontal viscosity terms for momentum; K_H is the vertical diffusivity for density; and F_ρ is the horizontal diffusivity term for density.

The pressure at depth z is obtained by integrating Eq. (3) vertically from z to the surface, η as follows:

$$p(x, y, z, t) = p_{\text{atm}} + g\rho_o\eta + g\int_z^0 \rho(x, y, z', t)\, dz', \quad (6)$$

where p_{atm}, atmospheric pressure, is assumed constant.

The terms in the dynamic equations related to small-scale horizontal mixing processes, not directly resolved by the model, are parameterized as

$$F_x = \frac{\partial}{\partial x}\left(2A_M\frac{\partial u}{\partial x}\right) + \frac{\partial}{\partial y}\left[A_M\left(\frac{\partial u}{\partial y} + \frac{\partial v}{\partial x}\right)\right], \quad (7)$$

$$F_y = \frac{\partial}{\partial y}\left(2A_M\frac{\partial v}{\partial y}\right) + \frac{\partial}{\partial x}\left[A_M\left(\frac{\partial u}{\partial y} + \frac{\partial v}{\partial x}\right)\right], \quad \text{and} \quad (8)$$

$$F_\rho = \frac{\partial}{\partial x}\left[A_H\frac{\partial \rho}{\partial x}\right] + \frac{\partial}{\partial y}\left[A_H\frac{\partial \rho}{\partial y}\right]. \quad (9)$$

Associated with the above five Eqs. (1)–(5) for the five unknowns u, v, w, p [i.e., η in Eq. (6)], and ρ are the initial and boundary conditions. However, A_M (con-

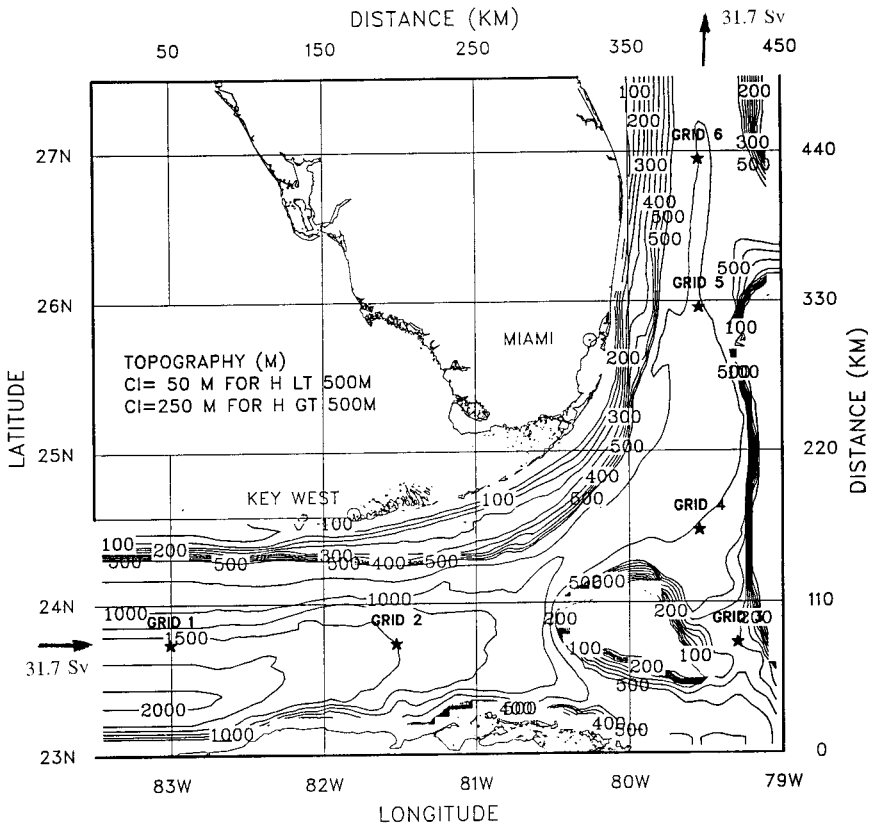

FIG. 1. The Straits of Florida and its topography (depth in m).

tained implicitly in F_x and F_y), A_H (contained implicitly in F_ρ), K_M, and K_H are four additional unknowns. Here K_M and K_H can be calculated using the Mellor–Yamada 2.5 turbulence closure model (Mellor and Yamada 1982). Horizontal viscosity and diffusivity, A_M and A_H, can be calculated according to Smagorinsky (1963):

$$A_M = C\Delta x\Delta y\left[\left(\frac{\partial u}{\partial x}\right)^2 + \left(\frac{\partial v}{\partial y}\right)^2 + \frac{1}{2}\left(\frac{\partial u}{\partial y} + \frac{\partial v}{\partial x}\right)^2\right]^{1/2}, \quad (10)$$

where Δx and Δy are the horizontal grid spacing in the x and y directions, respectively; and C is the nondimensional coefficient, which typically is of order of 0.1. However, the sophisticated turbulence parameterization formulas intrinsic to the model were temporarily replaced with constant eddy coefficients for the first generation NFS-COC, that is, $A_M = A_H = 50\ \text{m}^2\ \text{s}^{-1}$ and $K_M = K_H = 10^{-4}\ \text{m}^2\ \text{s}^{-1}$.

The bottom stress is determined by the following quadratic formula:

$$(\tau_{bx},\ \tau_{by}) = \left(\rho_o K_M\frac{\partial u}{\partial z},\ \rho_o K_M\frac{\partial v}{\partial z}\right) = C_B\rho_o(u_b^2 + v_b^2)^{1/2}(u_b,\ v_b), \quad (11)$$

where the subscript b denotes the bottom level, ρ_o is the water density, and $C_B = 0.0025$ is the nondimensional bottom drag coefficient.

The wind stress is determined by the following quadratic formula

$$(\tau_x,\ \tau_y) = \left(\rho_o K_M\frac{\partial u}{\partial z},\ \rho_o K_M\frac{\partial v}{\partial z}\right) = C_D\rho_A(W_x^2 + W_y^2)^{1/2}(W_x,\ W_y), \quad (12)$$

where W is the wind speed at 10 m above sea level, ρ_A is the air density, and $C_D = 0.0025$ is the nondimensional wind drag coefficient.

The finite-difference schemes used are centered differencing in space and leapfrog three-time stepping in time. Therefore, the Asselin (1972) filter is used every time step to remove the time-splitting noise or computational mode caused by the leapfrog scheme. Because one time step lag is used for the dissipation terms, the finite-difference schemes are of only first-order accuracy in time and of second-order accuracy in space (Wang 1996).

The model is established on a $4.5° \times 4.5°$ domain for the Straits of Florida, extending from the main inflow near the Dry Tortugas Island to the outflow near West Palm Beach (Fig. 1). The numerical grid has about 5.6 km $\times$ 5.6 km horizontal resolution that is eddy-resolv-

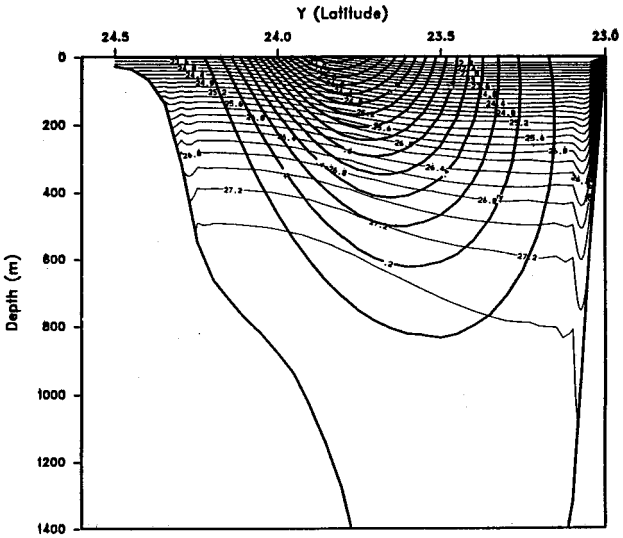

FIG. 2. The density distribution and the computed geostrophic flow at the western inflow open boundary at 83.5°W. The intervals of density and velocity are 0.2 kg m^{-3} and 10 cm s^{-1}, respectively.

ing, and there are 21 sigma levels. The time steps are 10 s for the barotropic/external model and 5 min for the baroclinic/internal mode. Realistic bottom topography is used to incorporate major features of the Straits; for example, Cay Sal Bank and the Miami Terrace (Fig. 1).

Annual Levitus climatology is used to specify the initial density field in the straits. First, the geostrophic current relative to the bottom at 83.5°W was calculated using density field (Fig. 2). Second, the total volume transport was adjusted to equal the 31.7 Sv annual mean transport of the Florida Current at 27°N (Leaman et al. 1987, 1989) by adding a barotropic transport uniformly across the strait. Third, the seasonal (cosine function) cycle with amplitude of 3 Sv (Lee et al. 1985) is superimposed into the total volume transport of 31.7 Sv. A radiation boundary condition is applied to the northern (outflow) boundary (Niiler and Richardson 1973; Leaman et al. 1987; Wang and Mooers 1997) to maintain volume transport conservation.

The computation of the geostrophic flow is conventional. However, the addition of barotrophic flow uniformly across the strait needs an iterative process by adding a small increment of the normal velocity at a time. Then, the volume transport is recomputed. This process is repeated until the difference is smaller than a certain value.

b. Trajectory model

A subgrid-scale turbulent dispersion model (a random walk Markovian stochastic process), surface wind drift, and the synoptic surface current predicted from POM model are used to predict the surface trajectory of a passive particle. Such ''random flight'' statistics for a particle was used in atmospheric dispersion by Pasquill and Smith (1983). Without wind forcing, Davis (1991) applied this model to ocean floats. Dutkiewicz et al. (1993) applied this model to the diffusion of particles in a meandering jet. In the following, the trajectory model is described with forcing by surface mean flow, surface wind drift, and turbulent velocity.

The Lagrangian motion of a particle in a two-dimensional plane in the presence of the instantaneous flow (U, V) forced by the real-time wind, a turbulent velocity (u, v), and surface wind forcing (W_x, W_y) is described with the following equations:

$$\frac{dx}{dt} = U + u + \alpha W_x, \qquad \frac{dy}{dt} = V + v + \alpha W_y, \quad (13)$$

where x and y are the particle trajectory coordinates at time t after the particle is released at a location (x_0, y_0) at time t_o. The turbulent velocity (u, v) is the complex and inherent motion that occurs at spatial and temporal scales much smaller than the predominant scales of the Florida Current and the wind drift surface current. This turbulent velocity is provided by a random number generator obeying a Gaussian distribution, with a mean of zero and a variance of unity. The turbulent velocity has only statistical meaning in contrast to the deterministic, large-scale motion (U, V) and wind drift motion (W_x, W_y). Here α is the wind factor (typically between 0.02 and 0.03). The random flight model that satisfies a well-mixed (homogeneous) condition and Gaussian turbulence (Thomson 1987) can be described as follows:

$$d\mathbf{v} = -\frac{1}{T}\mathbf{v}dt + K^{1/2}d\xi, \quad (14)$$

where T is the Lagrangian integration timescale (or turbulence decorrelation time) and the Lagragian correlation function is $\exp(-t/T)$, $K = 2\sigma^2/T$ is the turbulence diffusion coefficient, σ^2 is the variance of turbulence, and $d\xi$ is the stochastic kick received by the particle. The particle position and the turbulence velocity are jointly Markovian. The random flight model has been successfully applied to study some diffusion problems including small-scale atmospheric pollution dispersion (Thomson 1987) and ocean pollution (Wang 1999). For more details on this random flight statistical approach, see Thomson (1987) and Dutkiewicz et al. (1993).

There are two different ways to run the trajectory model. One uses operational (synoptic) Eta winds and the other uses the simulated (or idealized) winds. For the operational wind case, the NCEP Eta winds are extracted. For the research purpose, the idealized homogeneous wind is specified as a constant in both amplitude and direction at the sea surface. The surface currents are extracted at 1-m depth.

c. Simple data assimilation: Nudging to the volume transport

The nudging technique or Newtonian relaxation scheme (Anthes 1974; Hoke and Anthes 1976) is ef-

fective in reconstructing ocean circulation. It can be represented by the following formulation for north–south velocity, $v(x, y, z, t)$, in this case [actually valid for $u(x, y, z, t)$ in the dynamical equations] with inherent forcing $F(v, t)$:

$$\frac{\partial v}{\partial t} = F(v, t) + NG(t)(v_{\text{obs}} - v), \tag{15}$$

where the term on the left side is the local tendency of the north–south velocity at a specific model grid point in the domain, $F(v, t)$ contains all the physical forcing terms (linear and nonlinear terms of the prognostic evolution for v) present in the model. The coefficient N is the nudging coefficient, which determines how strongly the model equations are restored toward the observational data (N should be large enough to impact the assimilated analysis, and yet it must also be small enough to avoid exciting spurious modes in the model, such as the gravity and inertial modes), and $G(t)$, varying between 0 and 1, determines the forcing as a function of time, that is, the characteristics of the nudging cycles. Here $G(t)$ is used to slowly ''ramp up'' the data forcing as the time of the observation approaches, then gradually slows down the forcing as model integration moves beyond the observation period. This method leads to a smooth transition of particular data into and out of the assimilation process.

Integrating Eq. (15) with respect to x and z leads to

$$\frac{\partial V}{\partial t} = \int_{x,z} F(v, t)\, dx\, dz + NG(t)(V_{\text{obs}} - V), \tag{16}$$

where V is the north–south volume transport. In this case, the contribution of the integral of $F(v, t)$ of the volume transport may be negligible, because the baroclinic transport due to the vertical integration and nonlinear effect may be cancelled out by the integrations. Also, the volume transport is driven mainly by the barotropic inflow from the Gulf of Mexico and its value may have little relation to the inherent forcing, $F(v, t)$, thus, this term is reasonably neglected in this study.

Suppose that the observed volume transport, $V(t)$, is known as a function of time at 27°N, the following nudging method can be applied to the model at 27°N in every model integration time step:

$$V_{\text{mod}}^{n+1} = V_{\text{mod}}^{n-1} + 2NG(t)(V_{\text{obs}}^{n} - V_{\text{mod}}^{n})\Delta t, \tag{17}$$

where V_{obs} and V_{mod} denote the observed and modeled volume transport, respectively. In this study, V_{obs} was specified as the annual mean (31.7 Sv) plus seasonal cycle (±3 Sv). Actually, this method can be applied to any transect with available transport data, such as the Florida Current cable (real time) observations.

To find the timescale of N, we assume that N is constant and $G(t) = 1$, then we have

$$\frac{\partial V}{\partial t} = N(V_{\text{obs}} - V), \qquad \text{or}$$

$$V = V_0 e^{-Nt} + Ne^{-Nt} \int_0^t e^{Nt} V_{\text{obs}}\, dt, \tag{18}$$

where $t = 0$ represents the beginning of the preforecast period and V_0 is the value of V at $t = 0$. If $V_{\text{obs}}(t)$ is assumed to be constant in time toward which V is nudged, the solution to (17) is

$$V_{\text{mod}} = V_{\text{obs}} + (V_{\text{mod},0} - V_{\text{obs}})e^{-Nt}. \tag{19}$$

Thus, V_{mod} approaches the observed value V_{obs} as time passes, although never reaching it in finite time $T = N^{-1}$. Because NFS-COC conducts a 2-day forecast and the error is expected to decay exponentially to about 4% in $T = 3$ h (i.e., $NT = \pi$), then we set $N = 2.9 \times 10^{-4}$ s^{-1}.

The nudging procedure is described as follows. 1) At very model time step, the volume transport was calculated at 27°N by integrating north–south component of velocity with respect to x and z. 2) The nudging was performed using the third term of (17). 3) The model transport at time $n - 1$ [the second term of (17)] was adjusted by adding or subtracting the assimilated value [the third term of (17)] uniformly (with respect to x and z) to 2D (V) velocity field, and then 3D (v) velocity field, respectively, at all grids at 27°N. Since the model produces the vertical structure (with x and z distribution, see Wang and Mooers 1997) by itself, even though the nudging equation imposes a velocity change at all the grids at 27°N uniformly without any x–z structure, this minor change does not affect any of the original x–z structure of the current.

3. Documentation of the NFS-COC

a. Flowchart of the system controlled by the C-shell scripts

Figure 3 shows the flowchart and basic idea of NFS-COC, which is controlled and automatically executed by a number of C-shell scripts in the UNIX system. The details of the scripts can be referred to Wang (1999).

There are two subsystems, one for data capture and the other for the nowcast/forecast model run. Two subsystems are executed independently and sequentially. The data capture subsystem is to acquire and process the Eta Model surface wind from the NOAA Information Center (NIC)/NMC.

The data capture subsystem has a driver in the C-shell script, GetEta, which connects all the scripts related to acquiring the Eta model wind as listed below.

1) PinNIC: to check NIC server to see whether it is alive or down
2) LisEta: to acquire a list of products from NIC
3) ChStat: to check the status and list of products for the updated Eta wind

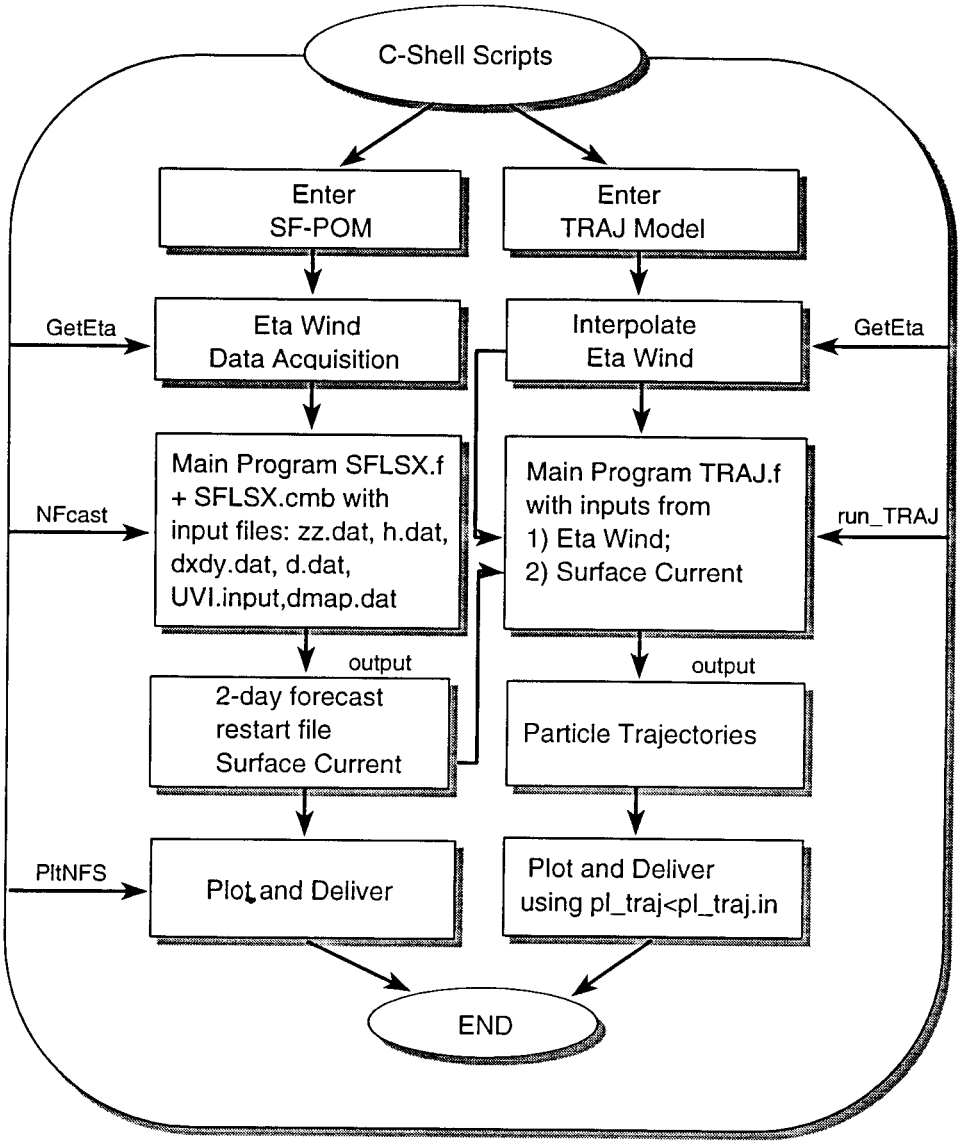

FIG. 3. The flowchart of NFS-COC controlled by the C-shell scripts, which enable NFS-COC to be a nearly fully automatic system.

4) FtpEta: to acquire the updated Eta wind
5) UpkEta: to decode Eta wind files
6) ItpEta: to interpolate Eta wind onto POM model grid
7) PltEta: to plot Eta wind and distribute plots
8) ArcEta: to archive Eta wind data

The nowcast/forecast subsystem is a driver in C-shell script, which includes the model calculation and delivery of the outputs, such as,

1) NFcast: to find the latest restart file and the latest Eta nowcast/forecast wind, and to run POM. Also, NFcast extracts the surface currents from the model outputs
2) PltNFS: to plot surface current superimposed with Eta wind vector and to distribute plots (PostScript files) to users.

If readers are interested in the details of the C-scripts as described, please refer the to appendices of Wang (1999).

b. Initialization, bottom topography, and inflow boundary condition

In this version, the density field is calculated prognostically. The initial annual climatological density field is obtained from Levitus data. The model uses realistic topography (Fig. 1). The inflow transport of 31.7 Sv for the Florida Current to the west (at 83.5°W) is calculated

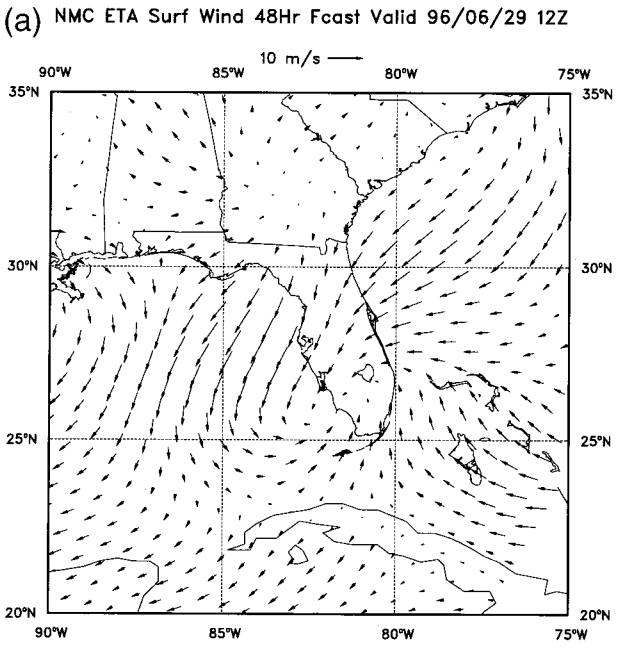

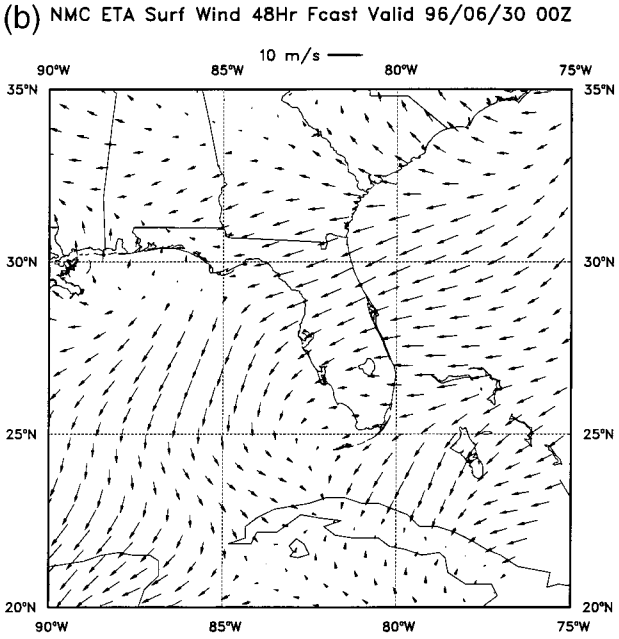

FIG. 4. The NFS-COC-downloaded Eta Model–predicted wind fields at (a) 1200 UTC 29 Jun and (b) 0000 UTC 30 Jun 1996.

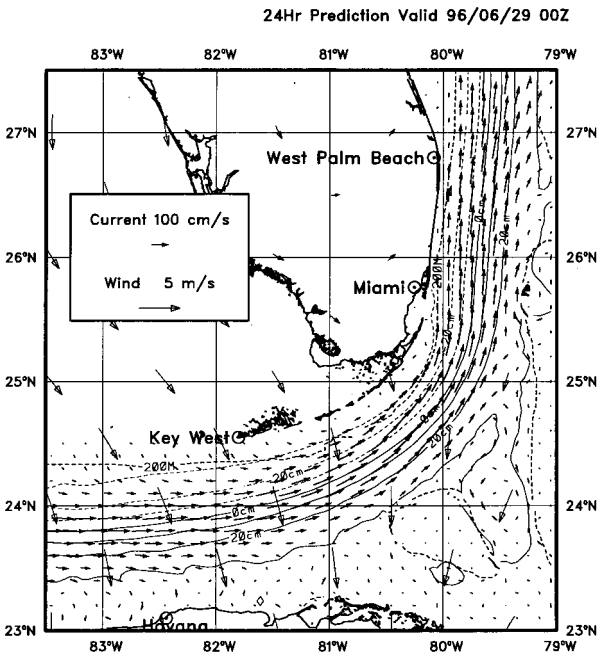

FIG. 5. The NFS-COC-predicted surface current and sea surface elevation under forcing of the Eta wind (open vectors) and the Florida Current at 0000 UTC 29 Jun 1996.

based on the geostrophic relation (Fig. 2). The outflow boundary condition specifies outward radiation to the north. For simplicity, this version omits the inflows (i.e., open boundaries) from Old Bahama Channel (~1.8 Sv) and NW Providence Channel (~1.2 Sv). Instead the total inflow of 31.7 Sv was specified at 83.5°W. In reality, the total annual volume transport of 31.7 Sv consists of the inflows from the Gulf of Mexico (~28.6 Sv) and two other inflows from Old Bahama Channel (~1.8 Sv) and NW Providence Channel (~1.2 Sv) (Leaman et al. 1995). The previous day model variables were saved as the restart (initialization) for the next day forecast. NFS-COC is automatically run for a 2-day forecast at 0000 EST every day on a Sun workstation.

c. Eta model wind output and decoding

To correctly maintain the system, a warning system has been established before each substep, when downloading (by ftp) Eta wind data is executed in order. When any step of the system does not finish normally, an outgo-mailing system issues error messages to the monitor screen of the system manager to indicate which step is not properly finished.

At least two times per day, the system downloads Eta wind data through the Internet automatically. If the system cannot find the new Eta wind or fails to connect to the file server at NCEP, the system will issue another request 1 h later.

All steps for downloading Eta winds include a dialog file. These dialog files record the actions being performed during each downloading execution. If an error occurs, the system manager needs to pay attention only to those dialog files to find the source of the error. For convenience, each dialog file includes information from both the current and previous step in the downloading process.

The system also includes an auto-mail warning system. If a problem is encountered during normal system operation, the system will issue a warning mail to the system manager. For example, PinNIC checks the NIC

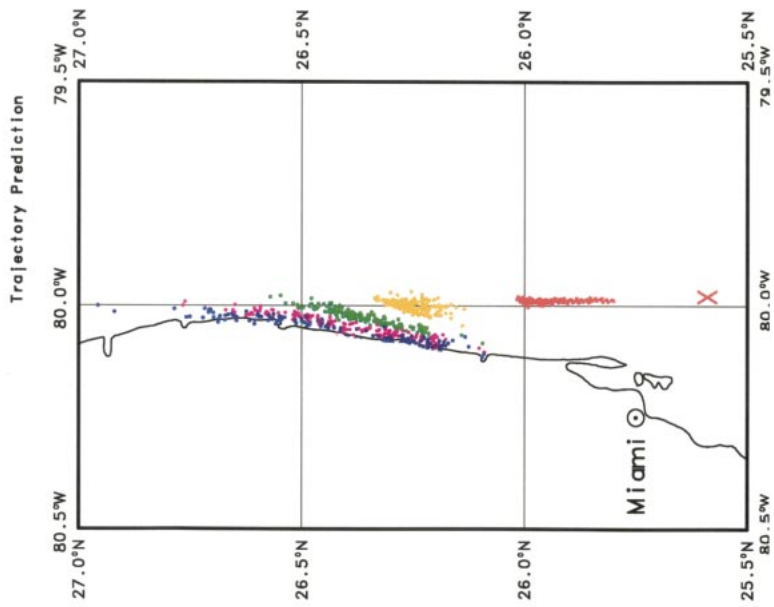

FIG. 7. The same as in Fig. 6 except that the idealized easterly wind of 5 m s^{-1} is applied homogeneously in space.

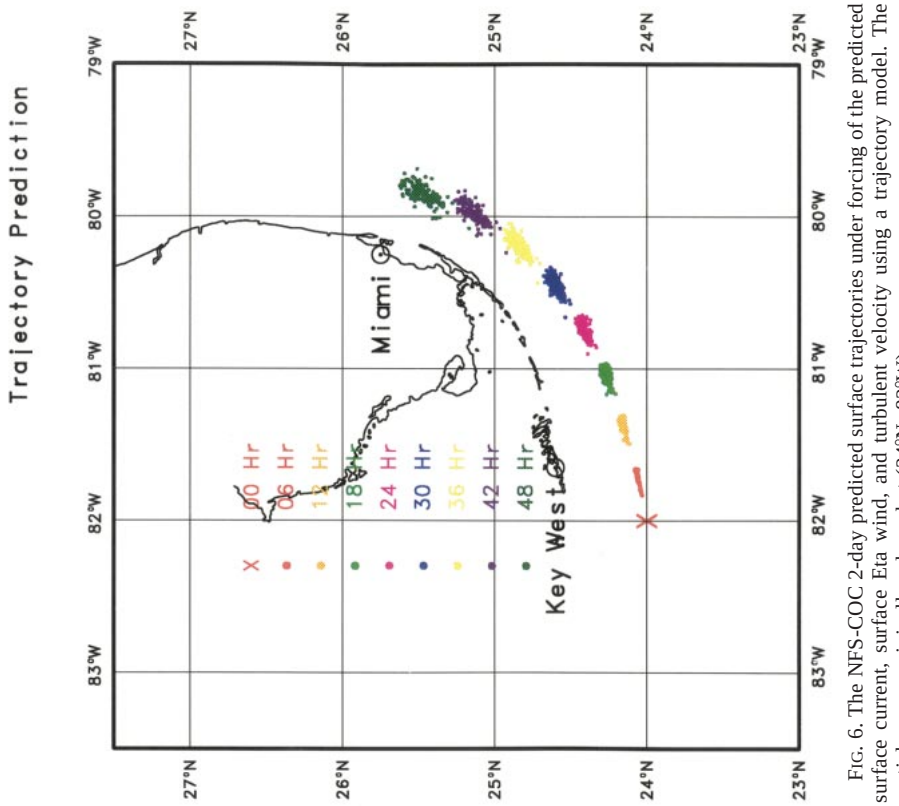

FIG. 6. The NFS-COC 2-day predicted surface trajectories under forcing of the predicted surface current, surface Eta wind, and turbulent velocity using a trajectory model. The particles were originally released at (24°N, 82°W).

server to see whether it is down or alive. LisEta obtains a list of products from NIC/NCEP.

d. The system prediction output (archival, network, and graphics)

In the fully automated NFS-COC, predicted outputs are generated every day. The system can be controlled by C-shell scripts to archive automatically the generated data files, compress the older files, and delete the oldest files. This can be seen in C-shell script NFcast (Wang 1999).

The graphics are generated using NCAR Graphics (actually they can be generated by many graphic software programs). The products are automatically sent to the users, executed by the C-shell script PltNHC.

4. NFS-COC products

To show that the NFS-COC has been working fairly satisfactorily since April 1994, we next present some predicted results and discuss these products. The model validation with observations can be referred to Wang and Mooers (1997) and Wang (1999).

a. Common nowcast/forecast products

The 3-day Eta Model wind prediction was downloaded automatically and the data in a subdomain (20°–35°N and 90°–70°W) were extracted from 0000 UTC 29 June to 1200 UTC 1 July 1996 (Fig. 4, only the maps of 1200 UTC 29 June 1996 and 0000 UTC 30 June 1996 are shown). The synoptic features and sea-breeze pattern in the wind fields were obvious, based on both direction and magnitude. Over the Straits of Florida, the wind was from south at about 3 m s^{-1} at 1200 UTC 29 June (Fig. 4a). However, at 0000 UTC 30 June (12 h later), the wind was flowing from the northeast at about 5 m s^{-1} (Fig. 4b). At 0000 UTC 1 July the northeasterly dominated over the region, while the easterly dominated 12 h later, that is, at 1200 UTC 1 July (not shown).

The 6-hourly, 3-day wind fields were further subinterpolated onto the NFS-COC domain (see Fig. 1) in the 5.6-km grids. The nowcast (not shown) and 2-day forecast of surface current and surface elevation, with the model wind vectors (coarse empty arrows) superimposed, at 0000 UTC 29 June 1996, were illustrated (Fig. 5). The energetic Florida Current with about 32 Sv inflow enters from the western boundary and exits through the northern boundary. Obviously, the Florida Current dominates and the wind forcing is secondary (Lee et al. 1985). These results show the synoptic wind variation from day to day with no drastic change, unlike a cold front or tropical cyclone passage. A detailed analysis of the Florida Current transport, potential vorticity balance, and its dynamical properties has been conducted (Wang and Mooers 1997) using NFS-COC.

Note that the model does not produce any frontal eddies and meanders because the sloping topography substantially suppresses the baroclinic instability (see Wang and Ikeda 1997). The meandering diminishes as it moves downstream (Lee 1997, personal communication). The mesoscale eddy growth rate was also calculated for the Florida Current, which is almost zero (see Fig. 5 of Wang 1999).

Figure 6 shows the 2-day prediction of particle trajectories under forcing of the surface current, surface Eta wind, and turbulent velocity as described above. The 150 particles prescribed by the user are released at 24°N, 82°W. As the particles are advected and dispersed downstream, particle density decreases. Thus, the particles diverge gradually downstream, which is attributed to the random turbulent (dispersion) velocity included in the model. Another simulation of release of the particles forced by an idealized easterly wind of 5 m s^{-1} is shown in a subdomain (Fig. 7). The trajectories released off Miami (around 25.6°N, 79.9°W) reach the coast about 1 day later. The results indicate that NFS-COC is capable of predicting possible trajectory path under realistic forcing although no direct observations have been made. If an oil spill event occurs in this region at any time, we have the capability to predict the possible oil spill path and possible consequences, which can help decision-makers plan their response to the pollutants.

b. A case for a late summer hurricane, Lili, during 16–20 October 1996

To capture an entire life cycle of a hurricane, the NFS-COC's products during Hurricane Lili (16–20 October) are presented below. This was a late summer hurricane. Unlike most years, 1996 had a heavier-than-normal hurricane season with the season lasting into mid-October. The tropical storm, Lili, was upgraded to hurricane on 17 October and hit Central America hard. The top sustained winds were near 90 mph with gusts as high as 115 mph. The moving speed was about 14 mph on 18 October. Hurricane Lili left thousands homeless and stranded more as rain-gorged rivers made bridges and roads impassable in Costa Rica, Honduras, and Nicaragua.

Figure 8 shows the Eta Model wind prediction products, which clearly monitored the evolution of Hurricane Lili during the period of 16–20 October (only the maps of 0000 UTC 18 October 1996 and 1200 UTC 19 October 1996 are shown). The hurricane center moved from the Strait of Florida (0000 UTC 18 October 1996) northeastward to the Bahama Islands (1200 UTC 19 October 1996). NFS-COC nowcasted and forecasted the surface ocean current patterns during the same period (Fig. 9, only the map of 0000 UTC 18 October 1996 is shown). NFS-COC again functioned well and provided users with updated information during the hurricane seasons in the Straits of Florida.

Pronounced features during the passage of Hurricane

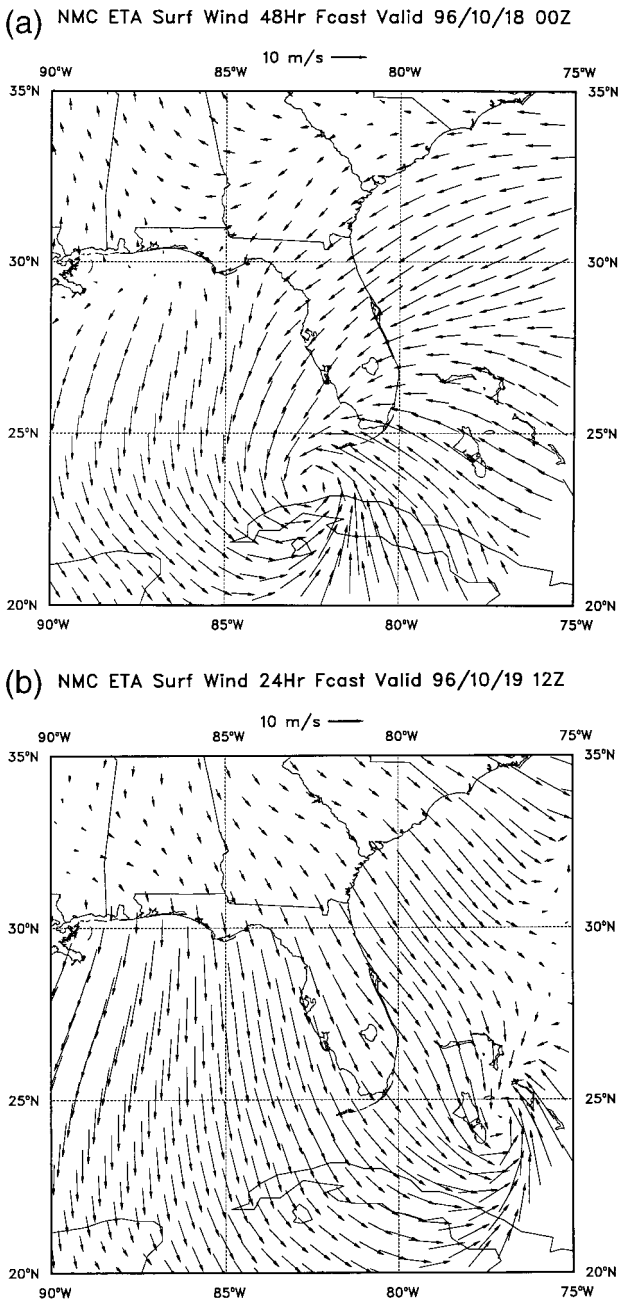

FIG. 8. The NFS-COC-downloaded Eta Model–predicted wind fields at (a) 0000 UTC 18 Oct and (b) 1200 UTC 19 Oct 1996, during the passage of Hurricane Lili.

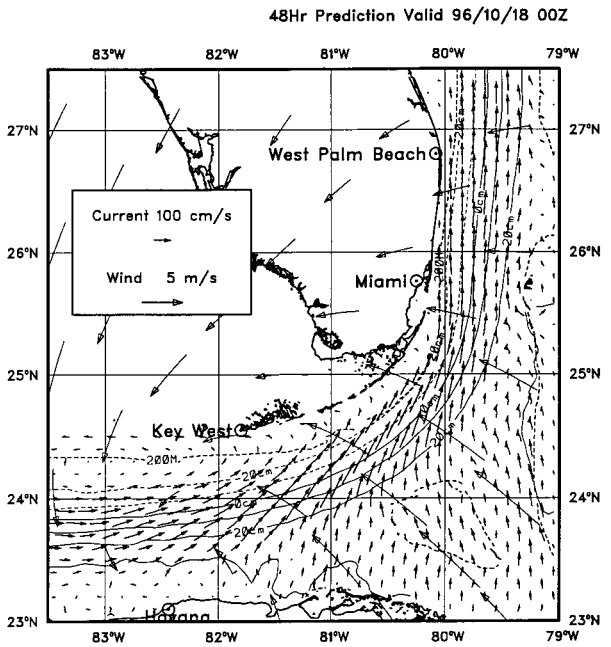

FIG. 9. The NFS-COC-predicted surface current and sea surface elevation under forcing of the Eta wind (open vectors) and the Florida Current at 0000 UTC 18 Oct 1996, during the passage of Hurricane Lili.

Lili were observed: 1) an elongated cyclonic circulation was excited near Key West (Fig. 9), which was not observed with no cyclonic hurricane (Fig. 5); and 2) surface currents in the southeastern region were much stronger than those with no high winds (Fig. 5).

5. Concluding remarks

In the above sections, the establishment of NFS-COC has been described in detail. The use of C-shell scripts enabled the automation of this system without much maintenance. This system is very practical and useful in the coastal oceans and will be applied to Prince William Sound, Alaska (Wang et al. 1997) in the near future. This system may be also applied to the Intra-America Sea, the Sea of Japan, etc., to help people understand the substantial progress made in ocean nowcast/forecast technique, taking advantage of the further advanced techniques in meteorology.

An improvement of this system will be achieved by second generation NFS-COC (Wang and Mooers 1997), which uses the Mellor–Yamada 2.5 turbulence closure model (Mellor and Yamada 1982) and Smagorinsky (1963) lateral friction closure. The vertical resolution increases from 21 levels in this version to 25 levels and two more realistic open boundaries are included in a research model (Wang and Mooers 1997). Furthermore, temperature and salinity will be treated as independent prognostic variables. The horizontal resolution may be increased from the present 5.6 to 2.8 km. The model domain will be extended to include the vast shallow coastal region off the western Florida coast, where fishery, industry, biological, and chemical processes are of main concern.

A near-real-time NFS-COC eventually will include sophisticated data assimilation of all the possible observed data into the model. These data include coastal sea levels, telemetered current data, SST, and sea surface heights from satellites, etc. Then, we will be able to say that ocean prediction techniques have advanced to a nowcast/forecast phase, like weather forecasts.

The important contribution of this study is, for the first time, the provision of the documented development of NFS-COC, using a simple nudging data assimilation scheme with many modern technical details in the Unix system. Building upon this prototype system, users can apply NFS-COC to many other coastal seas, semienclosed seas (such as the South and East China Seas, the Yellow Sea, the Bohai Gulf, the Sea of Japan, the Sea of Okhotsk, the Bering Sea, etc.) and even the Arctic Ocean. The products will be provided to users, such as fishermen, navigators, coast guard personnel, etc.

Acknowledgments. The author appreciates the financial support of the U.S. Coast Guard and NOAA, Exxon Valdez Oil Spill (EVOS) Trustees Council Alaska, and International Arctic Research Center (IARC)-Frontier Research System for Global Change (FRSGC). Valuable discussions with Drs. E. Rogers, and D.-S. Ko are gratefully acknowledged. The author also sincerely appreciates two anonymous reviewers for their very constructive comments, which helped improve the presentation of the paper.

REFERENCES

Anthes, R. A., 1974: Data assimilation and initialization of hurricane prediction models. *J. Atmos. Sci.,* **31,** 702–718.

Asselin, R., 1972: Frequency filter for time integrations. *Mon. Wea. Rev.,* **100,** 487–490.

Black, T. L., 1994: NMC notes: The new NMC mesoscale Eta Model: Description and forecast examples. *Wea. Forecasting,* **9,** 265–278.

Blumberg, A. F., and G. L. Mellor, 1987: A description of a three-dimensional coastal ocean circulation model. *Three-Dimensional Coastal Ocean Models.* N. S. Heaps, Ed., Vol. 4, *Coastal and Estuarine Sciences,* Amer. Geophys. Union, 1–16.

Brooks, I. H., and P. P. Niiler, 1975: The Florida Current at Key West: Summer, 1972. *J. Mar. Res.,* **33,** 1.

Davis, R. E., 1991: Observing the general circulation with floats. *J. Mar. Res.,* **38** (Suppl.), S531–S571.

Duing, O., and D. Johnson, 1971: Southward flow under the Florida Current. *Science,* **173,** 428–430.

Dutkiewicz, S., A. Griffa, and D. B. Olson, 1993: Particle diffusion in a meandering jet. *J. Geophys. Res.,* **98,** 16 487–16 500.

Hoke, J. E., and R. A. Anthes, 1976: The initialization of numerical models by a dynamic initialization technique. *Mon. Wea. Rev.,* **104,** 1551–1556.

Johns, W. E., and F. Schott, 1987: Meandering and transport variations of the Florida Current. *J. Phys. Oceanogr.,* **17,** 1128–1147.

Leaman, K. D., and R. L. Molinari, 1987: Topographic modification of the Florida Current by Little Bahama and Great Bahama Banks. *J. Phys. Oceanogr.,* **17,** 1724–1736.

——, ——, and P. S. Vertes, 1987: Structure and variability of the Florida Current at 27°N: April 1982–July 1984. *J. Phys. Oceanogr.,* **17,** 565–583.

——, E. Johns, and T. Rossby, 1989: The average distribution of volume transport and potential vorticity with temperature at three sections across the Gulf of Stream. *J. Phys. Oceanogr.,* **19,** 36–51.

——, R. L. Molinari, L. P. Atkinson, T. N. Lee, P. Hamilton, and E. Waddell, 1995: Transport, potential vorticity and current/temperature structure across Northwest Providence and Santaren Channels and the Florida Current off Cay Sal Bank. *J. Geophys. Res.,* **100,** 8561–8569.

Lee, T. N., and A. Mayer, 1977: Low-frequency current variability and spin off eddies on the shelf off southeast Florida. *J. Mar. Res.,* **35,** 193–220.

——, and E. William, 1988: Wind forced transport fluctuations of the Florida Current. *J. Phys. Oceanogr.,* **18,** 937–946.

——, F. A. Schott, and R. Zantopp, 1985: Florida Current: Low-frequency variability as observed with moored current meters during April 1982 to June 1983. *Science,* **227,** 298–302.

Mayer, D. A., K. D. Leaman, and T. N. Lee, 1984: Tidal motions in the Florida Current. *J. Phys. Oceanogr.,* **14,** 1551–1559.

Mellor, G. L., 1996: Users guide for a 3-D, primitive equation, numerical ocean model. Princeton University, 39 pp. [Available from Atmospheric and Oceanic Sciences Program, Princeton University, Princeton, NJ 08540.]

——, and T. Yamada, 1982: Development of a turbulence closure model for geophysical fluid problem. *Rev. Geophys. Space Phys.,* **20,** 851–875.

Molinari, R. L., W. D. Wilson, and K. Leaman, 1985: Volume and heat transport of the Florida Current: April 1982 through August 1983. *Science,* **227,** 295–297.

Mooers, C. N. K., and J. Wang, 1998: On the implementation of a 3-D circulation model for Prince William Sound, Alaska. *Contin. Shelf Res.,* **18,** 253–277.

Niiler, P. P., and W. S. Richardson, 1973: Seasonal variability of the Florida Current. *J. Mar. Res.,* **31,** 144–167.

Pasquill, F., and F. B. Smith, 1983: *Atmospheric Diffusion.* 3d ed. Halsted Press, 437 pp.

Rogers, E., D. G. Deaven, and G. J. DiMego, 1995: The regional analysis system for the operational ''early'' Eta model: Original 80-km configuration and recent changes. *Wea. Forecasting,* **10,** 810–825.

Schott, F., T. N. Lee, and R. Zantopp, 1988: Variability of structure and transport of the Florida Current in the period range of days to seasonal. *J. Phys. Oceanogr.,* **18,** 1209–1230.

Smagorinsky, J., 1963: General circulation experiments with the primitive equations. Part 1: The basic experiment. *Mon. Wea. Rev.,* **91,** 99–164.

Thomson, D. J., 1987: Criteria for the selection of stochastic models of particle trajectories in turbulent flow. *J. Fluid Mech.,* **180,** 529–556.

Wang, J., 1996: Global linear stability of the 2-D shallow water equations: An application of the distributive theorem of roots for polynomials on the unit circle. *Mon. Wea. Rev.,* **124,** 1301–1310.

——, 1999: A nowcast/forecast system for coastal ocean circulation (NFS-COC) using data assimilation. International Arctic Research Center–Frontier Research Program for Global Change Rep. 99-1, University of Alaska, Fairbanks, Fairbanks, Alaska, 97 pp.

——, and M. Ikeda, 1996: A 3D ocean general circulation model for mesoscale eddies-I: Meander simulation and linear growth rate. *Acta. Oceanol. Sin.,* **15,** 31–58.

——, and ——, 1997: Diagnosing ocean unstable baroclinic waves and meanders using quasi-geostrophic equations and Q-vector method. *J. Phys. Oceanogr.,* **27,** 1158–1172.

——, and C. N. K. Mooers, 1997: Three-dimensional perspectives of the Florida Current transport, potential vorticity, and related dynamical properties. *Dyn. Atmos. Oceans,* **27,** 135–149.

——, L. A. Mysak, and R. G. Ingram, 1994: A 3-D numerical simulation of Hudson Bay summer circulation: Topographic gyres, separations and coastal jets. *J. Phys. Oceanogr.,* **24,** 2496–2514.

——, C. N. K. Mooers, and V. Patrick, 1997: A three-dimensional tidal model for Prince William Sound, Alaska. Vol. 3, *Computer Modelling of Seas and Coastal Region,* J. R. Acinas and C. A. Brebbia, Eds., Computational Mechanics Publications, 95–104.